Turkish Journal of Chemistry

http://journals.tubitak.gov.tr/chem/

Research Article

Turk J Chem
(2014) 38: 372 – 380

doi:10.3906/kim-1212-40

PW_{12}-APTES@MCF: effective nanosized mesoporous composites for the oxidation of benzyl alcohols

Razieh FAZAELI[1,*], Hamid ALIYAN[2], Somaieh Parishani FOROUSHANI[1], Zahra MOHAGHEGHIAN[1]

[1]Department of Chemistry, Shahreza Branch, Islamic Azad University, Iran
[2]Department of Chemistry, Mobarakeh Branch, Islamic Azad University, Iran

Received: 15.12.2012 • **Accepted:** 23.07.2013 • **Published Online:** 14.04.2014 • **Printed:** 12.05.2014

Abstract: The surface of mesocellular silica foam (MCF) was modified by grafting 3-aminopropyl-triethoxysilane (APTES) to have a positive charge, and thus to provide sites for the immobilization of $H_3PW_{12}O_{40}$ (PW_{12}). This modified nanosized mesoporous silica (PW_{12}-APTES@MCF) was characterized by FTIR, XRD, BET, and TEM. XRD and adsorption–desorption analysis shows that the mesostructure of silica remains intact after various modifications, while the spectral technique shows the successful grafting of the neat PW_{12} inside the porous silica support. The oxidation of alcohols occurs effectively and selectively with H_2O_2 as the oxidant. PW_{12}-APTES@MCF was used as the catalyst. The catalyst can be reused several times but it will be less active.

Key words: Mesocellular silica foam (MCF), heterogeneous catalysis, polyoxotungstate

1. Introduction

Since ordered mesoporous silicas, KSW-1[1] and MCM-41,[2,3] were reported for the first time in the 1990s, many other mesoporous silicas with various pore geometries, such as MCM-48,[3,4] SBA-15,[5,6] SBA-16,[6–8] KIT-6,[9] FDU-12,[10] and MCF[11] have been synthesized and characterized chiefly by low-angle powder X-ray diffraction (XRD), transmission electron microscopy (TEM), and N_2 adsorption/desorption. The structure of the mesopores in KIT-6, similar to MCM-48,[4] is body-centered cubic, space group $Ia3d$. Pure siliceous KIT-6 material has an electronically neutral framework and is consequently devoid of Brönsted and Lewis acid sites. In order to improve the catalytic activity of this material, one must incorporate heteroatoms into the framework either by grafting or by direct synthesis. However, it is very difficult to prepare aluminum incorporated KIT-6 by direct synthesis under strongly acidic conditions due to dissolution of the aluminum source.[12]

Hydrogen forms (or free acids) of heteropoly acids (HPAs) usually have low surface areas (the drawbacks to the $H_3PW_{12}O_{40}$ (PW_{12}) and $H_3PMo_{12}O_{40}$ (PMo_{12}) are their low surface area, 1–5 $m^2\ g^{-1}$, and low porosity, $<0.1\ cm^3\ g^{-1}$). Supported heteropoly acid catalysts have much greater surface areas. Many attempts have been made to disperse and fix HPA catalysts on various supports. Support materials such as silica, carbon, and organic resins have been applied with varying levels of success, with new supporting materials and methods being actively pursued.[13–15]

Oxidation of alcohols into the corresponding aldehydes and ketones is one of the most fundamental

*Correspondence: fazaeli@iaush.ac.ir

transformations in organic synthesis. Usually, the oxidation of benzylic alcohols has been carried out using oxidants such as chromium(VI) trioxide,[16] nitric acid,[17] dimethyl sulfoxide/HBr,[18] and hypervalent iodine compounds,[19] Na_2WO_4,[20] and SBA-15-WO_4^{2-}.[21] In recent years, replacement of toxic oxidants in organic reactions has become of high priority in environmentally benign chemistry. Among other reagents, hydrogen peroxide is a cheap and easily available oxidizing reagent, and it is considered the most desirable oxidant in terms of environmental promoted oxidation of benzylic alcohols.

As part of a continuing effort to understand the catalytic properties of HPAs,[13–15] herein we report PW_{12}-APTES@MCF nanosized mesoporous composites as highly efficient catalyst in the presence of H_2O_2 for the aerobic oxidative of alcohols (Scheme 1).

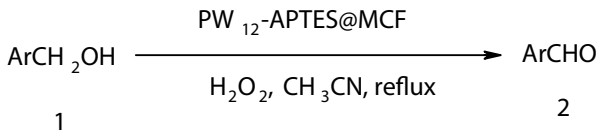

Scheme 1

2. Experimental

All materials were commercial reagent grade. Infrared spectra (400–4000 cm^{-1}) were recorded from KBr pellets on a PerkinElmer Spectrum 65 spectrometer. The X-ray powdered diffraction patterns were obtained on a Bruker D8 ADVANCE with automatic control. The patterns were run with monochromatic Cu Kα (1.5406 Å) radiation with a scan rate of 2° min^{-1}. Nitrogen adsorption measurements were performed at –196 °C by using an ASAP 2010M surface analyzer, and the pretreatment temperature was 180 °C. Transmission electron micrographs (TEMs) were obtained on a Jeol JEM 2010 scan-transmission electron microscope. The sample for the TEM measurement was suspended in ethanol and supported on a carbon-coated copper grid.

2.1. Preparation of MCF

The purely siliceous MCF sample was prepared as described previously[11] using a Pluronic P123 triblock copolymer ($EO_{20}PO_{70}EO_{20}$, Mav = 5800, Aldrich) surfactant with 1,3,5-trimethylbenzene (TMB) as the organic swelling agent with TMB/P123 = 0.5 (w/w). In a typical preparation, a solution of P123:TMB:1.6M HCl:TEOS = 2:1:75:4.25 (mass ratio) was prepared at room temperature and then heated to 40 °C. After 24 h at 40 °C, the milky reaction mixture was transferred to an autoclave and aged at 100 °C for another 24 h. The solid products were filtered off and dried overnight at 100 °C under static conditions. The occluded surfactant was removed by calcinations at 600 °C for 5 h in air, yielding the final mesoporous MCF material.

2.2. Preparation of PW_{12}-APTES@MCF

Scheme 2 shows the procedures for the surface modification of a mesoporous silica sample and the subsequent immobilization of $H_3PW_{12}O_{40}$ (PW_{12}) on the surface-modified mesoporous silica (APTES@MCF). Surface modification of mesoporous silica was done by a grafting method.[22]

To a suspension of 10 g of calcined mesoporous silica in 50 mL of dry toluene, 2.68 g of 3-aminopropyl triethoxy silane was added slowly and heated to reflux with continuous stirring for 8 h under nitrogen atmospheres. The powdery sample containing amino groups was filtered, washed with acetone, and then Soxhlet

extracted using a solution mixture of diethyl ether and dichloromethane (1:1) for 24 h and dried under vacuum. It was finally calcined at 180 °C for 2 h to yield the APTES@MCF. Immobilization of PW_{12} on the APTES@MCF was achieved as follows. APTES@MCF (1.0 g) was added to the acetonitrile solution containing 0.5 g of PW_{12} with vigorous stirring at room temperature, and the resulting solution was maintained at room temperature for 24 h. The solid product was filtered, and then it was dried overnight at 80 °C to yield the PW_{12}/APTES@MCF silica.[22]

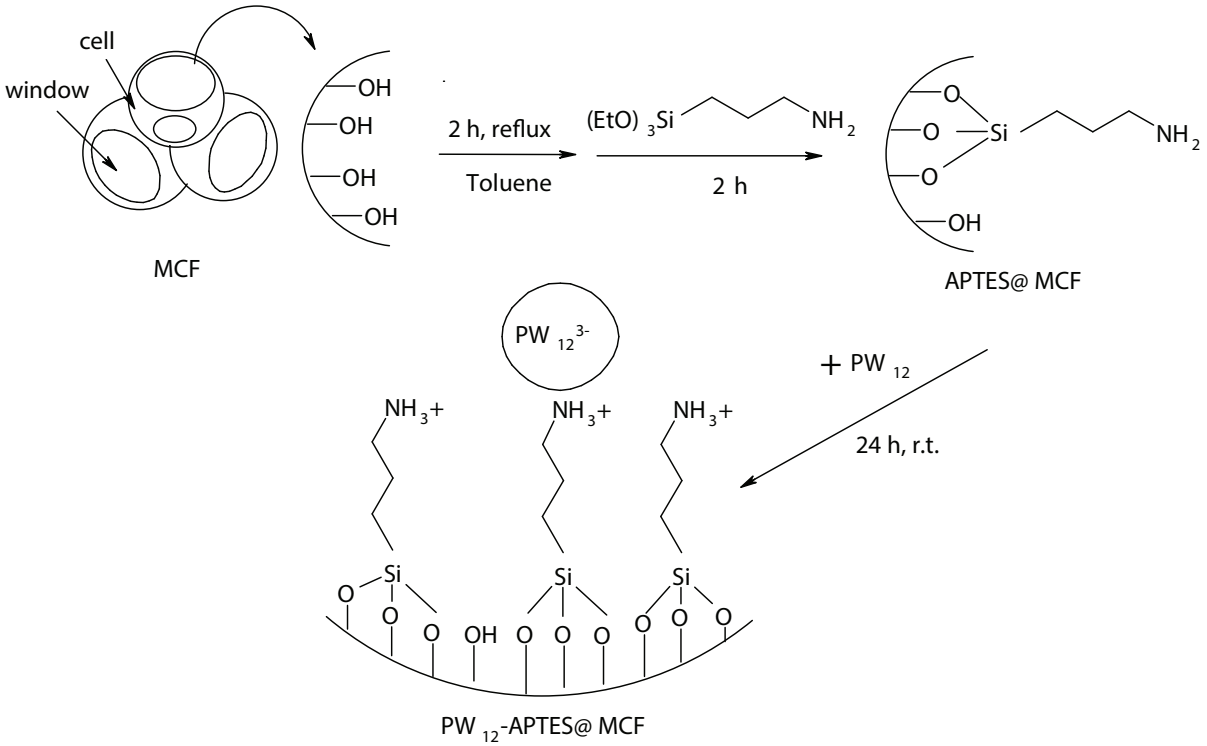

Scheme 2. The procedures for the surface modification of MCF and the subsequent immobilization of PW_{12} on the surface-modified MCF.

2.3. Oxidation of the benzylic alcohols: general procedure

A 25-mL round bottomed flask with 2 mL of CH_3CN equipped with a magnetic stirrer and reflux condenser was charged with 0.01 mmol catalyst and 5 mmol aqueous hydrogen peroxide (30%). The mixture was stirred and then 1 mmol alcohol was added. The biphasic mixture was stirred at 90 °C for the required time. Progress of the reaction was followed by aliquots withdrawn directly from the reaction mixture analyzed by GC using internal standard. After completion of the reaction, the mixture was treated with a 10% sodium hydrogen sulfite solution to decompose the unreacted hydrogen peroxide and then with 10% sodium hydroxide. The product was extracted with *n*-butyl-ether. The pure product was obtained by distillation or silica gel column chromatography (hexane/ethyl acetate, 10/1).

3. Results and discussion

3.1. Structural characterization

3.1.1. FTIR

Figure 1 presents the FTIR spectra in the skeletal region of 4000–400 cm^{-1} for the bare and modified mesoporous MCF materials. A band at 1624–1641 cm^{-1} observed in all samples can be assigned to the –OH vibration of physisorbed H_2O. In the case of MCF silica, APTES@MCF, and PW_{12}-APTES@MCF, the Si–O–Si bands that originated from MCF silica were observed at around 1097 cm^{-1} with a shoulder at 1250 cm^{-1} (due to asymmetric Si–O–Si stretching modes), 801–812 cm^{-1} (due to the corresponding symmetric stretch), 959 cm^{-1} (due to Si–O– or Si–OH), and 465 cm^{-1} (due to Si–O out-of-plane deformation).[23]

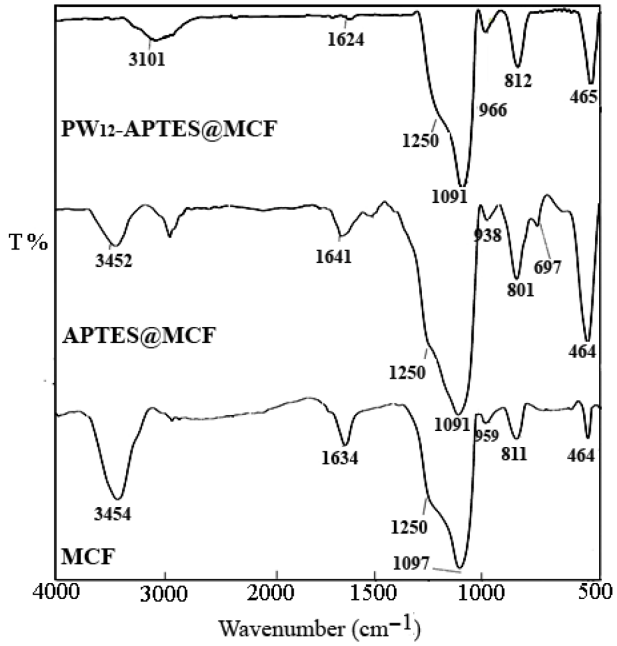

Figure 1. FTIR spectra of MCF materials.

The amino functionalization followed by succinylation of the mesoporous MCF silica was analyzed by FTIR spectroscopy. The broad band at 3600–3000 cm^{-1} for hydrogen bonded silanol[23,24] was appreciably reduced in the modified samples. The organosilane presence was identified by the absorbance of the band at 2950–2850 cm^{-1} for the propyl chain[23] and the deformation bands at 1455–1410 cm^{-1}.[25] The N–H absorption band overlapped with O–H bands at 3300–3500 cm^{-1}.[26] The presence of bands at 1710 cm^{-1} (C=O, acid), 1695–1650 cm^{-1} (C=O amide I band), 1566–1561 (NH amide II band), and 1415–1419 cm^{-1} (–C–N amide) confirmed that succinylation had taken place.[27] The successful immobilization of the PW_{12} catalyst on the aminopropyl-functionalized mesoporous silicas was confirmed by FT-IR analyses as shown in Figure 1. The primary structure of unsupported PW_{12} can be identified by the 4 characteristic IR bands appearing at 1080 cm^{-1} (P–O band), 990 cm^{-1} (W=O band), and 890 and 810 cm^{-1} (W–O–W bands).[28] The characteristic IR bands of PW_{12} in the PW_{12}/APTES@MCF were different from those of unsupported PW_{12}. The P–O band in the PW_{12}/APTES@MCF sample was not clearly identified due to overlap by the broad Si–O–Si band. However, W=O and W–O–W bands of PW_{12} in the PW_{12}/APTES@MCF appeared at slightly shifted

positions compared to those of the unsupported PW_{12}, indicating a strong interaction between PW_{12} and APTES@silica.[29]

3.1.2. XRD

Figure 2 shows the XRD patterns of the PW_{12}/APTES@MCF within the 2θ range of 0.7–10° (Figure 2a) and 0.7–10° (Figure 2b). There was no significant peak observed for MCF.[30] After immobilization of PW_{12}-APTES, the intensities of the reflections decrease, which could be assigned to the decrease in electron density contrast upon introduction of PW_{12}-APTES into the mesoporous of the silica host materials.

Figure 2b shows the XRD patterns of PW_{12}/APTES@MCF (2θ = 10–80°). It is interesting that the samples showed no characteristic XRD pattern, even though 35% wt% PW_{12} was loaded on the mesoporous silicas. This indicates that the PW_{12} species were not in a crystal state but in an amorphous-like state, demonstrating that Keggin species are finely and molecularly dispersed on the mesoporous silicas.

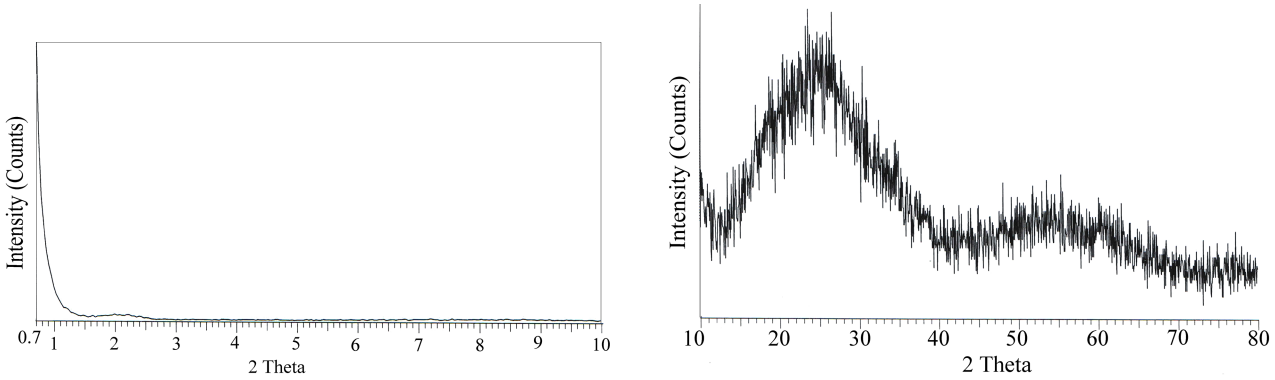

Figure 2. XRD patterns of PW_{12}-APTES@MCF (a) 2θ = 0.7–10°; (b) 2θ = 10–80°.

3.1.3. N_2 adsorption–desorption isotherms

Figure 3 shows the N_2 adsorption–desorption isotherms and pore size distributions of unmodified MCF and PW_{12}/APTES@MCF. All the samples exhibited typical IV-type isotherms and H1-type hysteresis loops at high relative pressures according to the IUPAC nomenclature,[31] which are typical characteristics of mesoporous materials.[32–34] This indicates that MCF mesoporous silica with large pore size distribution was successfully prepared. Interestingly, the PW_{12}/APTES@MCF showed a very similar isotherm pattern and pore size distribution (right) compared to bare MCF, indicating that the mesopore structure of mesoporous silica was maintained even after the surface modification step and the subsequent immobilization step of PW_{12}. Physical properties of parent MCF, PW_{12} (bulk), and modified MCF are listed in Table 1. As expected, the BET surface areas and total pore volumes of bare MCF are decreased after the functionalization with PW_{12}. These changes reflect that part of the mesopore volume in the MCF matrix is filled with PW_{12}.

Table 1. The texture parameters of bare MCF and PW_{12}-APTES@MCF in comparison with the bulk PW_{12} materials.

Entry	Sample	BET, surface area (m^2/g)	Pore volume (cm^3/g)	D_W (nm)[a]
1	MCF, silica	720	1.3	7.1
2	PW_{12}	6	-	-
3	PW_{12}/APTES@MCF	53	0.9	5.9

[a]Window diameter, D_W, determined according to the BJH method.

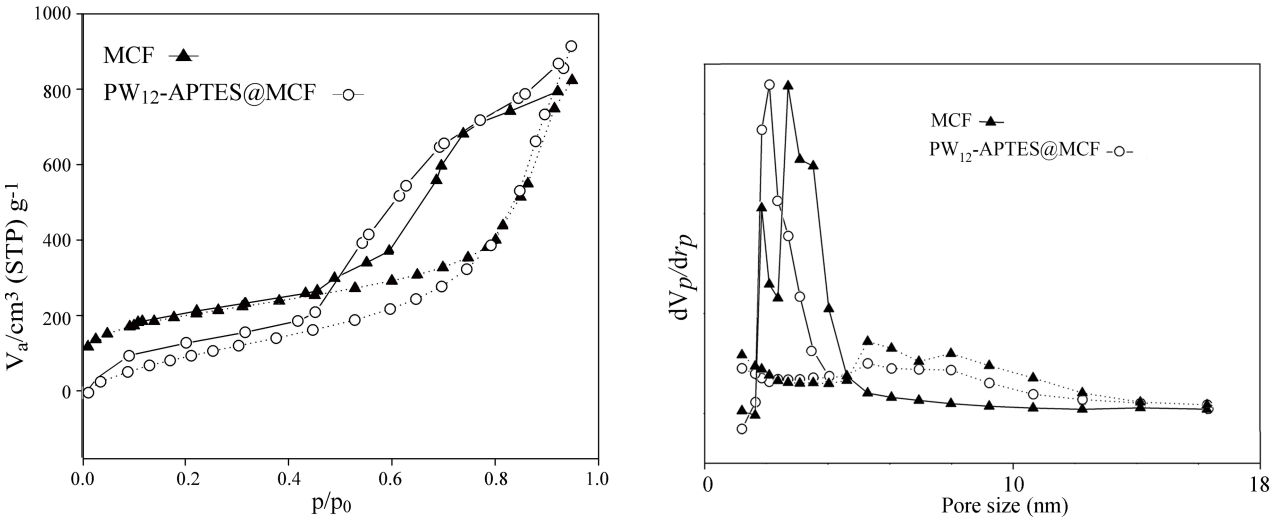

Figure 3. N_2-adsorption–desorption isotherms (a) and (b) pore size distributions calculated by the BJH method (right) of bare MCF and PW_{12}-APTES@MCF.

3.2. TEM

Figure 4 shows the TEM images of PW_{12}/APTES@MCF. The sample for the TEM measurement was suspended in ethanol and supported on a carbon-coated copper grid. PW_{12}/APTES@MCF catalyst exhibited a disordered pore structure with large pores in the range of 9–11 nm. A well-resolved contrast characteristic of certain silica mesopore structure symmetry is still observed, which is an indication of the preservation of the long ordered arrangement of the channels in the silica host matrix after PW_{12} deposition. The places with darker contrast could be assigned to the presence of PW_{12} particles with different dispersion. The small dark spots in the images could be ascribed to PW_{12} particles, probably located in the support channels. The larger dark areas over the channels most likely correspond to PW_{12} agglomerates on the external surface.[35,36]

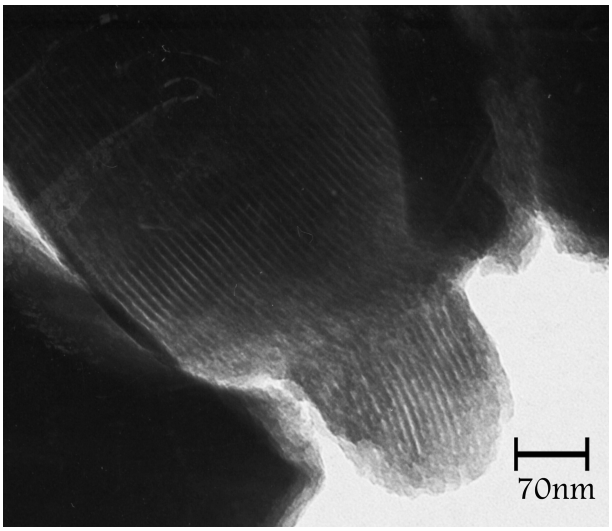

Figure 4. TEM image of PW_{12}-APTES@MCF.

3.3. Oxidation of benzylic alcohols

The catalytic activity of the prepared catalyst was tested using benzyl alcohols as reference alcohol. Oxidation was carried out with H_2O_2 as an oxidant and in the presence of catalytic amounts of PW_{12}-APTES@MCF. The optimum conditions used for the oxidation of benzyl alcohol by this catalytic system comprised substrate, oxidant, and catalyst in a mol ratio of 1:12:0.04, respectively (Table 2). In the catalytic reactions the choice of solvent is crucial. The influence of various solvents on the yield of the reaction was investigated using benzyl alcohol as the substrate. From these studies it was concluded that CH_3CN was the most favorable solvent (Table 2). The performance of the PW_{12}-APTES@MCF composite and MCF (bare) is shown in Table 2. It is important that PW_{12}-APTES grafting caused the increase in reactivity.

Table 2. Effect of different conditions in the oxidation of benzyl alcohol with catalytic amount of PW_{12}/APTES@MCF.[a]

Entry	Solvent	PW_{12}-APTES@MCF (mol %)	Yield (%)[b]
1	H_2O	4	62
2	CH_3CN	4	98
3	CH_2Cl_2	4	38
4	EtOH	4	53
5	MeOH	4	48
6	CH_3Cl	4	40
7	CH_3CN (25 °C)	4	60
8	CH_3CN (40 °C)	4	75
9	CH_3CN	3	25
10	CH_3CN	2	60
11	CH_3CN	4 (bare MCF)	75

[a] Reaction condition: benzyl alcohol (1 mmol), catalyst, H_2O_2 (12 mmol), solvent (5 mL); under reflux conditions after 20 min.
[b] Isolated yield.

To study the scope of this procedure, the oxidation of other alcohols was studied next (Table 3). To test the role of electron influence of phenyl substituents on the efficiency of oxygenation, 4-MeO-benzyl alcohol and 4-NO_2-benzyl alcohol were exposed to the oxidation system. Conversion of these 2 substrates was 92% and 78% after 35 min and 70 min, respectively. The electron-withdrawing nitro group reduced the reactivity of benzyl alcohol toward oxidation, whereas the methoxy group at the para position of the phenyl ring increased the tendency of benzyl alcohol oxidation (Table 3). In addition, the yield of 2-NO_2-benzyl alcohol (Table 3, entry c) was lower than that of 2-OH-benzyl alcohol (Table 3, entry e).

The recovery and reusability of the catalyst were investigated (Table 4). We noted that after the addition of $CHCl_3$ to the reaction mixture this catalyst can be easily recovered quantitatively by simple filtration. The wet catalyst was recycled (the nature of the recovered catalysts was followed by ICP (Table 4)) and no appreciable change in activity was seen after 3 cycles.

Table 3. Oxidation of benzylic alcohols with UHP catalyzed by PW_{12}/APTES@MCF in CH_3CN at reflux conditions.[a]

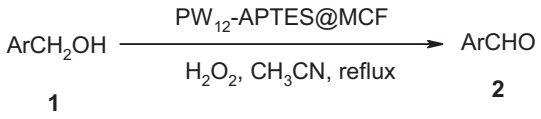

Substrate (**1**)	Ar	Product (**2**)	Time (min)	Yield (%)[b,c]
1a	C_6H_5	2a	20	98
1b	4-NO_2-C_6H_4	2b	70	78
1c	2-NO_2-C_6H_4	2c	50	75
1d	4-HO-C_6H_4	2d	30	92
1e	2-HO-C_6H_4	2e	20	95
1f	4-MeO-C_6H_4	2f	35	92
1g	4-Cl-C_6H_4	2g	30	92
1h	2-Cl-C_6H_4	2h	25	80
1i	4-F-C_6H_4	2i	70	78
1j	4-Br-C_6H_4	2j	45	75
1k	2-Me-C_6H_4	2k	25	92

[a] Reaction conditions: benzyl alcohol (1 mmol), catalyst (0.04 mmol), H_2O_2 (12 mmol), CH_3CN (5 mL) under reflux conditions.
[b] Isolated yield.
[c] Yield based on GC.

Table 4. Investigation of the feasibility of reusing of PW_{12}-APTES@MCF in the oxidation of benzyl alcohol.

Run	Yield (%)[a]	Amount of W leached (%)[b]
1	98	-
2	98	-
3	95	0.02
4	88	0.05
5	56	0.38

[a] Isolated yield.
[b] Determined by ICP.

4. Conclusions

The results of this research demonstrated that PW_{12}-APTES@MCF affects catalysts for aerobic oxidation of benzylic alcohols using H_2O_2. The advantages of this catalytic system are mild reaction conditions, short reaction times, moderate to good product yields, easy preparation of the catalysts, nontoxicity of the catalysts, and simple and clean work-up of the desired products.

Acknowledgment

We gratefully thank Shahreza Branch, Islamic Azad University, for its financial support.

References

1. Yanagisawa, T.; Shimizu T.; Kuroda, K. *Bull. Chem. Soc. Jpn.* **1990**, *63*, 988–992.
2. Kresge, C. T.; Leonowicz, M. E.; Roth, W. J. *Nature* **1992**, *359*, 710–712.

3. Beck, J. S.; Vartuli, J. C.; Roth, W. J. *J. Am. Chem. Soc.* **1992**, *114*, 10834–10843.
4. Monnier, A.; Schuth, F.; Huo, Q. *Science* **1993**, *261*, 1299–1303.
5. Zhao, D. Y.; Feng, J. L.; Huo, Q. S. *Science* **1998**, *279*, 548–552.
6. Zhao, D. Y.; Huo, Q. S.; Feng, J. L. *J. Am. Chem. Soc.* **1998**, *120*, 6024–6036.
7. Sakamoto, Y.; Kaneda, M.; Terasaki, O. *Nature* **2000**, *408*, 449–453.
8. Ravikovitch, P. I.; Neimark, A. V. *Langmuir* **2002**, *18*, 9830–9837.
9. Kleitz, F.; Choi, S. H.; Ryoo, R. *Chem. Commun.* **2003**, 2136–2137.
10. Fan, J.; Yu, C. Z.; Gao, T. *Angew. Chem. Int. Ed.* **2003**, *42*, 3146–3150.
11. Lettow, J. S.; Han, Y. J.; Schmidt-Winkel, P.; Yang, P.; Zhao, D.; Stucky, G. D.; Ying, J. Y. *Langmuir* **2000**, *16*, 8291–8295.
12. Prabhu, A.; Kumaresan, L.; Palanichamy, M.; Murugesan, V. *Appl. Catal. A: Gen.* **2009**, *360*, 59–65.
13. Fazaeli, R.; Tangestaninejad, S.; Aliyan, H. *Appl. Catal. A: Gen.* **2007**, *318*, 218–226.
14. Fazaeli, R.; Aliyan, H. *Appl. Catal. A: Gen.* **2007**, *331*, 78–83.
15. Fazaeli, R.; Aliyan, H. *Appl. Catal. A: Gen.* **2009**, *353*, 74–79.
16. Hajipour, A. R.; Mallakpour, S. E.; Khoee, S. *Synlett* **2000**, 740–742.
17. Strazzolini, P.; Runcio, A. *Eur. J. Org. Chem.* **2003**, 526–536.
18. Li, C.; Xu, Y.; Lu, M.; Zhao, Z.; Liu, L.; Cui, Y.; Zheng, P.; Ji, X.; Gao, G. *Synlett* **2002**, 2041–2042.
19. Surendra, K.; Krishnaveni, N. S.; Reddy, M. A.; Nageswar, Y. V. D.; Rao, K. R. *J. Org. Chem.* **2003**, *68*, 2058–2059.
20. Noyori, R.; Aoki, M.; Sato, K. *Chem. Commun.* **2003**, 1977–1986.
21. Zhang, R.; Ding, W.; Tu, B.; Zhao, D. *Chem. Mater.* **2007**, *19*, 4379–4381.
22. Chaube, V. D.; Shylesh, S.; Singh, A. P. *J. Mol. Catal: Chem.* **2005**, *241*, 79–87.
23. Diaz, I.; Marquez-Alvarez, C.; Mahino, F.; Perez-Periente, J.; Sastre, E. *J. Catal.* **2000**, *193*, 283–294.
24. Wouters, B. H.; Chen, T.; Dewilde, M.; Grobet, P. J. *Micropor. Mesopor. Mater.* **2001**, *44–45*, 453–457.
25. Jarzebski, A. B.; Szymańska, K.; Bryjak, J.; Mrowiec-Białoń, J. *Catal. Today* **2007**, *124*, 2–10.
26. Guo, Y.; Li, D.; Hu, C.; Wang, Y.; Wang, E.; Zhou, Y.; Feng, S. *Appl. Catal. B: Env.* **2001**, *30*, 337–349.
27. Aburto, J.; Ayala, M.; Bustos-Jaimes, I.; Montiel, C.; Terrés, E.; Domínguez, J. M.; Torres, E. *Micropor. Mesopor. Mater.* **2005**, *83*, 193–200.
28. Kozhevnikov, I. V. *Catalysis by Polyoxometalates*, Wiley: Chichester, UK, 2002.
29. Chaube, V. D.; Shylesh, S.; Singh, A. P. *J. Mol. Catal. A: Chem.* **2005**, *241*, 79–87.
30. Kannan, K.; Jasra, R. V. *J. Mol. Catal. B: Enzym.* **2009**, *56*, 34–40.
31. Sing, K. S. W.; Everett, D. H.; Haul, R. A. W.; Moscou, L.; Pierotti, R. A.; Rouquerol, J. *Pure Appl. Chem.* **1985**, *57*, 603–619.
32. Beck, J. S.; Vartuli, J. C.; Roth, W. J.; Leonowicz, M. E.; Kresge, C. T.; Schmitt. K. D. *J. Am. Chem. Soc.* **1992**, *114*, 10834–10843.
33. Kresge, C. T.; Leonowicz, M. E.; Roth, W. J.; Vartuli, J. C.; Beck, J. S. *Nature* **1992**, *359*, 710–712.
34. Che, M.; Védrine, J. C. *Characterization of Solid Materials and Heterogeneous Catalysts: From Structure to Surface Reactivity,* Wiley-VCH: Weinheim, Germany, 2012, 853–879.
35. Tsoncheva, T.; Ivanova, L.; Rosenholm, J.; Linden, M. *Appl. Catal. B: Env.* **2009**, *89*, 365–374.
36. Castner, D. G.; Watson, P. R.; Chan, I. Y. *J. Phys. Chem.* **1989**, *93*, 3188–3194.